Author/s:
Crombie, ML;Lisé-Pronovost, A;Giansiracusa, MJ;Boskovic, C;Roberts, A;Lauer, F;Popelka-Filcoff, RS

Title:
A new method for fingerprinting ochre sources using mineral magnetic measurements

Date:
2025-07-01

Citation:
Crombie, M. L., Lisé-Pronovost, A., Giansiracusa, M. J., Boskovic, C., Roberts, A., Lauer, F. & Popelka-Filcoff, R. S. (2025). A new method for fingerprinting ochre sources using mineral magnetic measurements. Journal of Archaeological Science, 179, pp.106222-106222. https://doi.org/10.1016/j.jas.2025.106222.

Persistent Link:
https://hdl.handle.net/11343/356491

Journal of Archaeological Science 179 (2025) 106222

Contents lists available at ScienceDirect

Journal of Archaeological Science

journal homepage: www.elsevier.com/locate/jas

A new method for fingerprinting ochre sources using mineral magnetic measurements

Maddison L. Crombie [a,b,*], Agathe Lisé-Pronovost [a], Marcus J. Giansiracusa [b], Colette Boskovic [b], Amy Roberts [c], Felix Lauer [a], River Murray and Mallee Aboriginal Corporation [d], Rachel S. Popelka-Filcoff [a]

[a] School of Geography, Earth and Atmospheric Sciences, University of Melbourne, Victoria, 3010, Australia
[b] School of Chemistry, University of Melbourne, Victoria, 3010, Australia
[c] Archaeology, College of Humanities, Arts and Social Sciences, Flinders University, South Australia, 5402, Australia
[d] c/o Berri, South Australia, 5343, Australia

A B S T R A C T

Fingerprinting of iron-rich natural pigments commonly known as ochre, provides the opportunity to trace the cultural movement of these ochres in the archaeological past. This manuscript presents a proof-of-concept approach to the analysis and characterisation of ochre deposits, through the application of magnetic analytical methods. The use of measurements such as room temperature – saturation isothermal remnant magnetisation (RT-SIRM), isothermal magnetisation sweeps (hysteresis loops) and zero-field-cooled/field-cooled (ZFC-FC) remanence allow for the identification of a magnetic mineral profile in the ochre samples, which can, in turn, be used to fingerprint sources. Using low-temperature remanence and hysteresis measurements, we have demonstrated the ability to discriminate between geological contexts and thereby contribute to the greater goal of tracing cultural exchange via the movement of ochre from their original sources.

1. Introduction

Ochre has been used throughout history by cultures worldwide as a natural colour pigment, appearing in the archaeological record as early as 250 kya (Barham, 2002) and habitually as early as 140 kya (Wolf et al., 2018). Archaeologically and ethnographically, there is evidence for the use of ochre not only as a pigment in symbolic behaviour such as rock art, but also in a wide range of ritual and medicinal practices, playing a significant role in the lives of people of the past (Hodgskiss, 2020). Provenance studies trace the movement of these ochre pigments, yet some existing methodologies are limited in their ability to characterise or provenance ochres. However, the ochre itself presents an analytical challenge due to the inherent heterogeneity of the material.

Ochre is any rock, clay or soil rich in colouring iron oxides, with varying iron and metal oxides concentrations within and between deposits (Mastrotheodoros and Beltsios, 2022; Popelka-Filcoff et al., 2007). More broadly in the context of archaeology, the term ochre extends to the wide range of Fe-based natural pigments that are observed in the archaeological record as artefacts as well as known sources (Popelka-Filcoff and Zipkin, 2022). The ochre sources presented in this paper are geological deposit sites that are culturally significant for pigment procurement in the archaeological past as well as the present. The Fe-oxides and Fe-hydroxides found in most ochre pigments are responsible for the observed vibrant colours, with the red ochres containing mainly hematite (α-Fe_2O_3), yellow ochres mainly goethite (α-FeOOH), while magnetite (Fe_3O_4) can be red-brown in colour (Mastrotheodoros and Beltsios, 2022). For most ochre deposits the mineral composition is often a mixture of two or more iron oxides and/or iron hydroxides, usually resulting in colour variation that is further altered by their accessory minerals of clays and sands (Ward et al., 2001). The colour of the iron oxides themselves are impacted by particle size (e.g. nanosized hematite appears red and turns more purple with increasing particle size) (Mastrotheodoros and Beltsios, 2022; Schwertmann, 1993). Mineral magnetic measurements provide a unique opportunity to differentiate between the iron mineralogy of ochres.

Non-destructive methodologies for fingerprinting artefacts are popular among archaeological scientists due to ethical considerations relating to the imperative to preserve cultural materials (Pálsdóttir et al., 2019). However, there are few truly non-destructive methodologies. In contrast, mineral magnetic measurements are completely non-destructive when heating is not involved and are suitable for very small sample sizes (5–50 mg). To date, there have only been a small

This article is part of a special issue entitled: Worldwide Archaeological Science of Ochre published in Journal of Archaeological Science.

* Corresponding author. School of Geography, Earth and Atmospheric Sciences, University of Melbourne, Victoria, 3010, Australia.
E-mail address: crombie.m@unimelb.edu.au (M.L. Crombie).

https://doi.org/10.1016/j.jas.2025.106222
Received 14 October 2024; Received in revised form 19 March 2025; Accepted 7 April 2025
Available online 3 May 2025

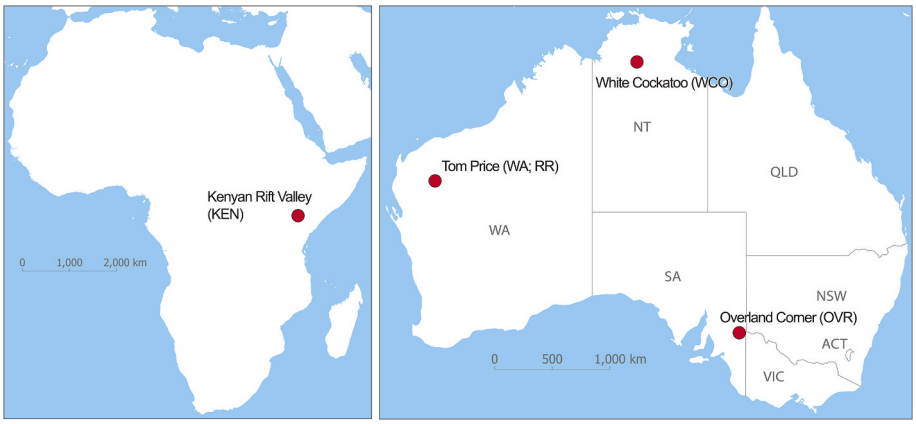

Fig. 1. Locations of ochre sources studied.

number of studies that have used environmental magnetism on ochres (i.e. Kukkonen et al. (1997), Mooney et al. (2003) and Tsatskin and Gendler (2016)). The use of mineral magnetic measurements to provenance ochres was first demonstrated by Mooney et al. (2003), where a combination of different measurements was utilised to fingerprint sites. This study determined that room temperature hysteresis loops, SIRM, anhysteric remnant magnetisation and magnetic susceptibility could provide absolute magnetisation values for the different measurement types, however multiple different magnetometers were required to collect these data. In addition, their ascription of the different iron oxide types to the ochres was done based on the colours of the sources (i.e. yellow ochres contain goethite and red contain hematite), rather than on the magnetic data. Further, the study did not address the major complexity of working with iron oxide containing ochres, which is that Fe-based pigments are often mixtures of multiple Fe-based minerals, and that ochres and their deposits are most often heterogenous in their composition.

This paper presents a novel method for characterising the iron oxide components of ochre pigments using a modified version of the measurement protocols by Lagroix and Guyodo (2017) to separate the magnetic mineralogy of complex natural mineral assemblages using low temperature experiments. The use of these methods allows for the identification of unique magnetic properties that can be attributed to the presence of magnetic minerals (mainly goethite, hematite and magnetite) that are found in complex samples such as iron-rich ochre pigments. These iron-bearing minerals can go undetected using other analytical methods such as X-ray diffraction (XRD) or Mössbauer spectroscopy due to the small amounts of minerals often found in bulk mixtures, while mineral magnetic measurements can detect magnetic minerals at concentrations as low as 1 ppm and are predominantly unaffected by the diamagnetic clay matrix that is often associated with ochres (Lagroix and Guyodo, 2017). The approach in this work maximises efficiency and data acquisition where a single instrument can perform all steps of the analysis, which is not possible with standard vibrating sample magnetometers (VSM). This approach reduces the amount of time spent measuring the sample and allows the user to deconvolute complex mixtures of iron oxides using room temperature (RT) and low temperature (LT) measurements (Appendix A). In doing so, mixed signals can be unmixed both qualitatively and, in some cases, quantitatively to reveal the dominant magnetic minerals and thus a fingerprint which can be attributed to the site or sample. In addition, this paper presents a new approach to the processing and interpretation of room temperature – saturation isothermal remnant magnetisation (RT-SIRM) measurements, particularly for the semi-quantitative determination of goethite concentration in mixtures.

2. Materials and methods

2.1. Archaeological source ochre samples

Source ochre samples were obtained from locations in Australia and in Kenya. Australian ochre samples were collected from three different geographical regions: White Cockatoo, Northern Territory; Tom Price, Western Australia and Overland Corner, South Australia (Roberts et al., 2022) (Fig. 1 and Table 1). These three ochre outcrop sites were chosen due to their archaeological and cultural significance and documentation (i.e. traditional quarry sites), their geographic and geological differences, and because of the strong research partnerships with the Aboriginal communities who collaborated on this project to enable seasonal access to the sites for re-sampling. The Northern Territory samples were collected by Aboriginal people from Barunga, Northern Territory, the Overland Corner samples collected with River Murray and Mallee Aboriginal Corporation (RMMAC) community members in South

Table 1
Summary of sources analysed in this study.

Site	Number of samples	Geological setting	Sample Description
Overland Corner	2	Weathered fine to medium sandstone of the Parilla Sands (Tertiary)(Roberts et al., 2022)	Yellow and red weathered sedimentary rock
Tom Price	3	WADP and WARE samples are from the banded and laminated Marra Mamba Iron Formation (Early Proterozoic)(Klein and Gole, 1981) RR samples are from the banded iron formation of the Brockman Iron Formation (Early Proterozoic)(Pickard, 2002)	Yellow and red weakly aggregated flakes
White Cockatoo	2	Cretaceous weathering surface in sedimentary rock (Sweet et al., 1994)	Surface ferricrete nodules, yellow and red mottled
Kenyan Rift Valley	2	Weathered and/or geothermally altered volcanic rocks (Quaternary) (Zipkin et al., 2017)	Soft to lithified alteration products (See Zipkin et al. (2017), Table 2)

Australia, and the Tom Price samples collected with Yinhawangka and Wintawari Guruma people in Western Australia. Within each site a set of subsites were defined, and within subsites samples were taken to allow the investigation into both intra-site and inter-site variation. Due to cultural permissions, exact locations and photos cannot be provided for these sites.

The Kenyan samples were from a collection of well-characterised ochres from the Kenyan Rift Valley (KRV), also representing sites which have archaeological significance (Zipkin et al., 2015, 2017). These samples were taken from three distinct volcanic regions along the KRV, the Mount Suswa Volcano, the Eburru Volcanic and the greater Olkaria Volcanic Complex. At each of the sites the ochre samples were taken to represent as much intra-site variation as possible, with the focus on obtaining a range of iron-based pigments (Zipkin et al., 2017).

The samples presented in this study have been selected to represent the variation in magnetic measurement data observed across a larger set of samples from each of the sites: Overland Corner, Tom Price, White Cockatoo, and Kenyan Rift Valley.

2.2. Mixture standards

To better understand the contribution and quantification of varying amounts of magnetic minerals in mixtures in archaeological ochre for RT-SIRM measurements, model pigments of varying amounts of hematite and goethite were prepared. Mineral standards for hematite and goethite were synthesised chemically in a laboratory based on protocols from literature (Jaiswal et al., 2013; Lassoued et al., 2017). Subsequently, mixtures of goethite and hematite were created by varying the amounts of each component (99:1, 95:5, 90:10, 75:25, 50:50, 25:75 goethite to hematite) to represent the likely concentration of goethite in the archaeological samples measured. XRD analysis was performed on each mixture to validate the concentration of each component (Appendix B and section 2.3).

2.2.1. Hematite synthesis

The synthesis of hematite was conducted using the precipitation method outlined by Lassoued et al. (2017). Solid $Fe(NO_3)_3{\cdot}9H_2O$ was used as a precursor and 2 M ammonia solution (NH_4OH) as a precipitating reagent. A sample of $Fe(NO_3)_3{\bullet}9H_2O$ (20.2 g, 0.05 mol) was hydrated in 1 L of RO water and heated to 80 °C. Ammonia solution was added dropwise after an initial addition of 50 mL until a pH of 11 was reached. The solution was stirred continuously for 3 h at 80 °C. The precipitate was filtered using vacuum filtration, washing with RO water. The paste was dried overnight in a 110 °C oven. In a furnace the powder was heated to 1100 °C for 4 h, resulting in a solid lump of hematite. This was ground into a powder using an agate mortar and pestle.

2.2.2. Goethite synthesis

The goethite synthesis was performed following the method outlined in Jaiswal et al. (2013) with the addition of further washing steps. Solid $Fe(NO_3)_3{\bullet}9H_2O$ was used as a precursor and 2.5 M potassium hydroxide (KOH) as a precipitating reagent. A sample of $Fe(NO_3)_3{\bullet}9H_2O$ (25 g, 0.06 mol) was hydrated in 250 mL of RO water, mixing for 24 h. Potassium hydroxide (KOH) solution was added (75 mL), then dropwise until a pH of 12 was reached. The solution was aged for 5 days in a 60 °C oven. After five days, the solution was washed with RO water six times to ensure the removal of any unreacted iron and potassium nitrate and vacuum filtered. The remaining goethite was dried for 24 h in a 60 °C oven and ground to a fine powder using an agate mortar and pestle.

2.2.3. Other standards

A geological magnetite sample was sourced from the South Australian Museum mineral collection. The commercially available pigment, "Yellow Ochre Dark" from Rublev Colours was measured as an Al-goethite standard.

2.3. X-ray diffraction (XRD)

The XRD data were collected using a Bruker D8 Advance Eco X-ray diffractometer with Co Kα radiation (1.7890 Å). The diffractometer was operated at a generator voltage of 35 kV and a current of 28 mA. The optics included a 0.6 mm divergence slit, a Fe-filter, and both primary and secondary 2.5° Soller slit. An anti-scattering knife was also used, which was positioned 7 mm above the sample surface. The data were collected in a 2θ range of 35–135° by Lynxeye XE position-sensitive detector in 1D mode, with a step size of 0.03° and a dwell time of 1.8 s per step, corresponding to 345.6 s per step with the 192-line detector strips. Mineral identification was done using DIFFRAC.TOPAS software to obtain quantitative phase analysis (Appendix B). Cobalt XRD was performed to quantify the amount of Al-goethite in the sample to ensure that no other iron oxides were present to alter the signal (Appendix B).

2.4. Colour measurements

The RGB colours of the nine archaeological samples were measured using a Spectro 1 colour measurement device (Appendix D, Fig. 2). 5–10 mg of pigment was mixed with 3–5 drops of water to create a paint and applied to a canvas. Colour measurements were taken from the centre of the dried paint squares.

2.5. Magnetic mineral analyses

2.5.1. Sample preparation

All ochre material was ground to a fine powder using an agate mortar and pestle. Approximately 30 mg of ochre powder was weighed into a polycarbonate gel capsule from AGC Chemicals. The capsule was then packed with cotton wool to ensure that the powders were restrained. Any additional materials used (i.e. scissors, spatulas and Kapton tape) were all non-magnetic to minimise the potential for contamination. A cotton blank was measured to confirm that all materials used were non-magnetic. Where samples could not be adequately restrained, eicosane was added, however this was avoided where possible due to the destructive nature of adding a binder to the ochres. The capsule was then mounted in a plastic straw. For the preparation of enhanced SIRM measurements between 5 and 30 mg of ochre powder was added to VSM powder sample holders from Quantum Design, which were then placed in a brass sample mount.

2.5.2. Superconducting quantum interference device (SQUID)

The characterisation of the ochres was performed on a Quantum Design MPMS3 SQUID magnetometer at the University of Melbourne. The protocol has been optimised from Lagroix and Guyodo (2017) to minimise measurement time while allowing high-resolution data to be collected. The full measurement protocol can be found in the Supplementary Information (Appendix A).

Hysteresis measurements were performed in a 7 T field with a sweep rate of 100 Oe/s to enhance the likelihood of magnetic saturation of the magnetic minerals, compared to routine environmental magnetism studies often limited to 1–2 T (eg. Liu et al. (2012)). However, in this

study no samples reached saturation, which is not surprising since goethite and hematite can remain non-saturated in fields as high as 57 T (Rochette et al., 2005).

The RT-SIRM measurements (Fig. 2) were performed with an initial applied field of 5 T. The field was then returned to 0 T and a magnet reset was performed in an attempt to remove any remanent field from the superconducting magnet. Small residual fields can remain after a magnet reset, and therefore remanence measurements may be biased with a small paramagnetic contribution if paramagnetic materials are present in the sample (Qian et al., 2021). Measurements were collected on cooling to 10 K with a step size of 4 K and a sweep rate of 2 K/min. The samples were then measured as they warmed back to room temperature using the same step size and sweep rate. This protocol probes how a sample's remanent magnetisation acquired at room temperature changes with temperature and enables mineralogical determinations based on the shape of the curves and temperature transitions (e.g., the Verwey transition (T_V) of magnetite and the Morin transition (T_M) of hematite (Dunlop and Özdemir, 1997; Jackson and Moskowitz, 2020)). Importantly, temperature transitions vary depending on stoichiometry and cation substitution. For example, in maghemite (oxidised magnetite) common in soils, the Verwey transition is often subdued or suppressed by surface oxidation (Özdemir et al., 1993). In the case of hematite, it has been shown that decreasing particle size and/or Al substitution lowers the temperature at which the transition occurs (Özdemir et al., 2008).

The zero-field-cooled, field-cooled (ZFC-FC) remanence measurements were performed by cooling the sample to 10 K then applying a field of 5 T, returning to 0 T and then resetting the magnet. The response was measured as the sample warmed to 300 K (ZFC) with a step of 4 K and sweep rate of 2 K/min. Following this a field of 5 T was applied and the sample was then cooled from 300 K to 10 K, then the field was returned to 0 T and a magnet reset was performed. The response was then measured when heating the sample from 10 K to 300 K (FC). A small number of samples were measured between 10 K and 320 K with a 2 K step, however this was later changed to reduce the measurement time. Similarly to RT-SIRM, the ZFC-FC protocol informs mineral determinations based on the shape of the curves and temperature transitions, but for remanent magnetisations acquired when cooling within a field. This is especially useful for identifying goethite, which is known to have higher moments in FC than ZFC due to the acquisition of remanence during the cooling process (Liu et al., 2006).

Enhanced SIRM measurements were performed as detailed by Lagroix and Guyodo (2017) whereby an initial acquisition of an IRM was achieved in a 5 T field at 300 K, the response monitored as the temperature was cycled from 300 K to 10 K, 10–400 K, 400 to 10 K and 10–300 K. This was done to identify the presence of goethite in the sample mixtures dominated by the presence of hematite and magnetite by cycling the temperature through its Néel temperature at 393 K (see Appendix D, Fig. 2).

2.5.3. Data manipulation

All data were mass-normalised and hysteresis parameters were calculated from HystLab without any drift or slope correction (Paterson et al., 2018). The first point for each ZFC and FC curve was removed prior to analysis as initial points were identified as artefacts from the cooling cycle. The Al-goethite sample was mass-corrected for the iron-oxide component (Al-goethite) as approximately 31 % of the total sample determined through quantitative XRD (Appendix B). Therefore, a calculated mass of 9.591 mg for the Al-goethite standard is used for all corrections rather than the original measured bulk mass of 30.94 mg.

3. Results and discussion

3.1. Low-temperature behaviour of iron oxide standards

The adapted method from Lagroix and Guyodo (2017) was applied to the synthesised hematite and goethite samples, their mixtures and the geological magnetite sample, producing a set of standard data which can be compared to the archaeological samples (Fig. 2). The resultant SIRM curve shapes are consistent with those presented by Lagroix and Guyodo (2017), however the absolute values for the magnetic parameters (Table 2) differ. The overall trend of the parameters is the same between the literature and this work (i.e. hematite is the most coercive mineral and magnetite is the least), and therefore the difference in absolute values likely represents the range of magnetisation values that can be observed for any given mineral (Özdemir and Dunlop, 2014). The coercivity (B_c) of the iron oxide standards is indicative of the force required to resist demagnetisation in the presence of a field. As a result of this, different iron oxides will produce either low-coercivity (closed) loops, open (high-coercivity) loops, or a mixture of these which can be useful tools to understand the domain states for the different iron oxides. In addition to the hematite, goethite and magnetite, Al-goethite was also measured to explain the variation observed in the source samples.

3.1.1. Hematite

Hematite is a high coercivity mineral characterised by a hysteresis loop open at high fields (up to about 2 T in Fig. 2). In low temperature thermomagnetic experiments, hematite is readily identifiable with low magnetic remanence at low temperatures and the Morin transition at 250 K ((Özdemir et al., 2008); Fig. 2). This phenomenon occurs as the antiferromagnetic hematite changes to weakly ferromagnetic at 250 K (Morin, 1950). The synthetised hematite has a magnetisation ratio (Mr/Ms = 0.125; Table 2) and coercivity (Bc = 260 mT; Table 2); values indicative of fine single domain (SD) nanosized particles (Özdemir and Dunlop, 2014), which likely resemble what is found in ochre.

3.1.2. Goethite

Goethite displays higher magnetic moments at low temperatures, reversible RT-SIRM and a large opening in ZFC-FC experiments (Liu et al., 2006). The coercivity (Bc = 39 mT; Table 2) is in the lower range of natural and synthetic goethite (e.g. Peters and Dekkers, 2003). Since magnetic coercivity is directly related to particle size in goethite (Peters and Dekkers, 2003), the low coercivity value suggests very fine particle sizes were synthetised, which aligns with archaeological ochre analysis.

3.1.3. Magnetite

Magnetite is a low-coercivity ferrimagnetic mineral characterised by strong magnetic memory and the Verwey transition (T_V) around 120 K (Jackson and Moskowitz, 2020). The geological magnetite sample displays a hysteresis loop saturated at a low field (<0.5 T; Fig. 2), which is the highest magnetic remanence of the standards analysed (Table 2) and T_V visible in RT-SIRM and ZFC-FC (Fig. 2). The closed hysteresis shape, low magnetisation ratio Mr/Ms (<0.02; Dunlop (2002)), and a ZFC curve above the FC curve (Kosterov, 2003) are indicative of large multi domain (MD) particles.

3.1.4. Al-goethite

The low temperature behaviour of Al-goethite closely resembles goethite in Fig. 2, except for a change in slope at temperatures >250 K (Fig. 2). In addition, Al-goethite returns higher magnetic moments, especially at low temperatures (Table 2). Al substitution in goethite decreases particle size and increases coercivity up to several hundreds of

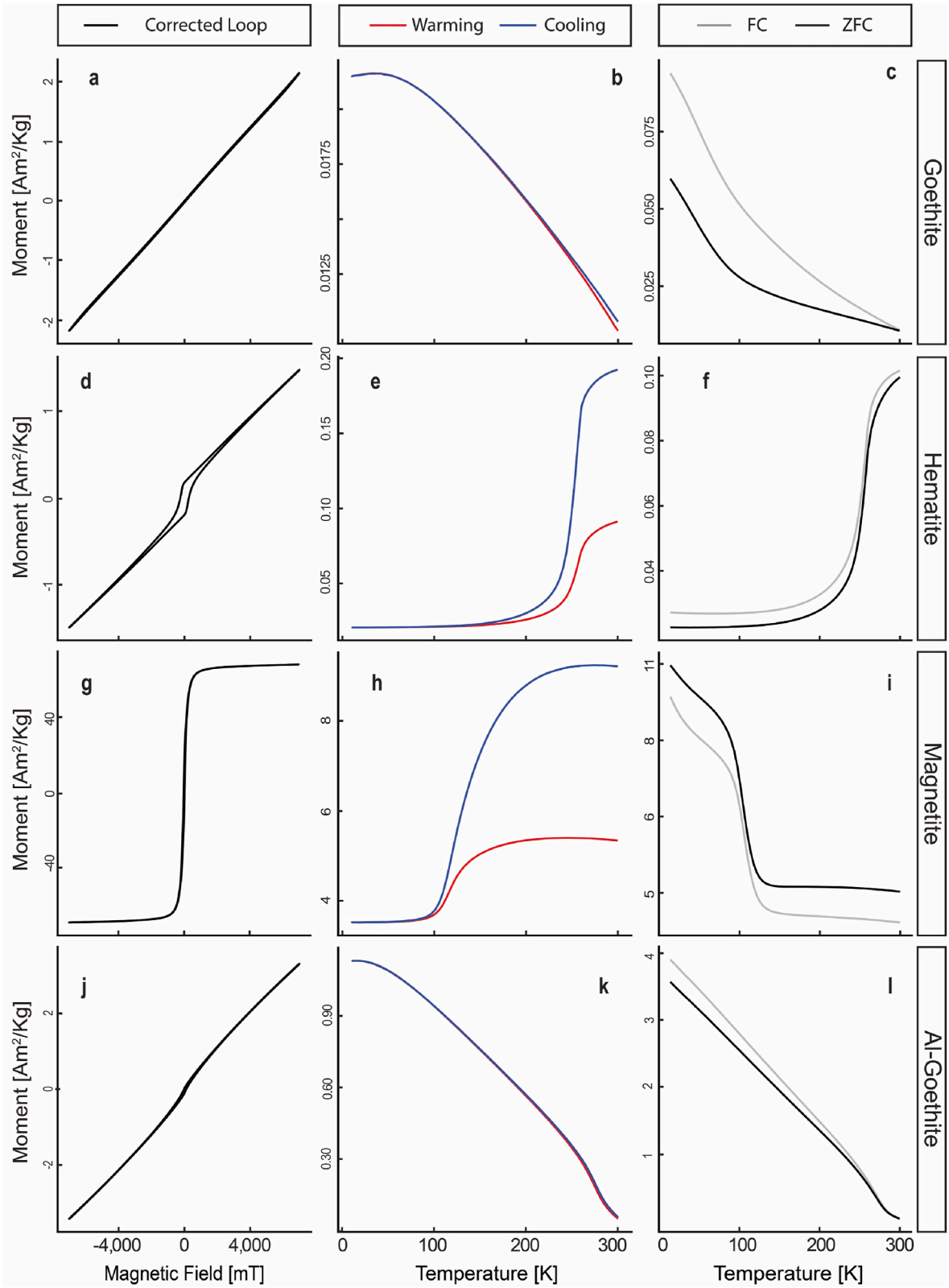

Fig. 2. Summary of magnetic data profiles for synthesised goethite, hematite, geological magnetite and Al-goethite samples. (Left) hysteresis loops, (middle) RT-SIRM and (right) ZFC-FC.

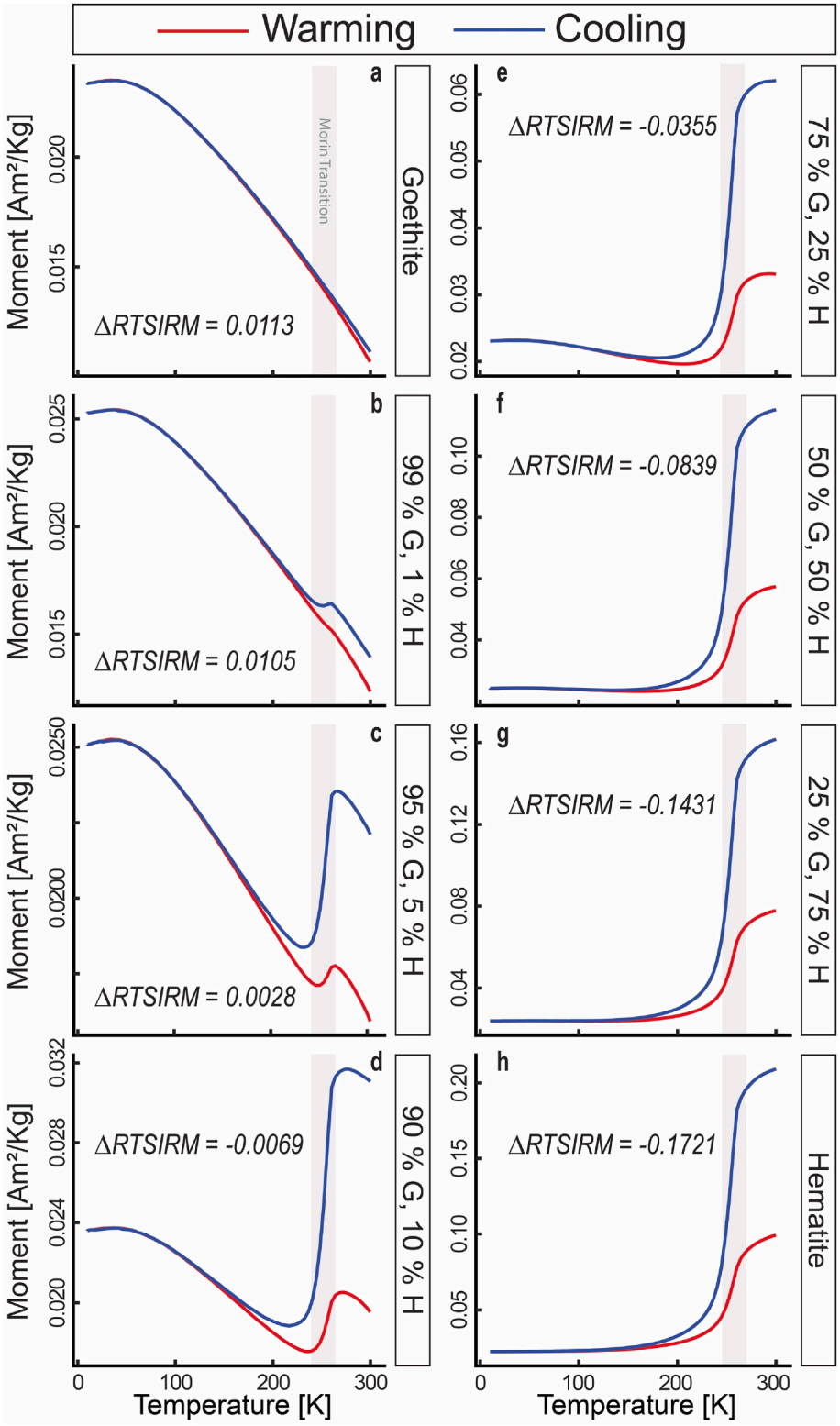

Fig. 3. RT-SIRM measurements for goethite and hematite mixture standards. Grey bars denote the range in which the Morin transition occurs (241–261 K) (Özdemir et al., 2008).

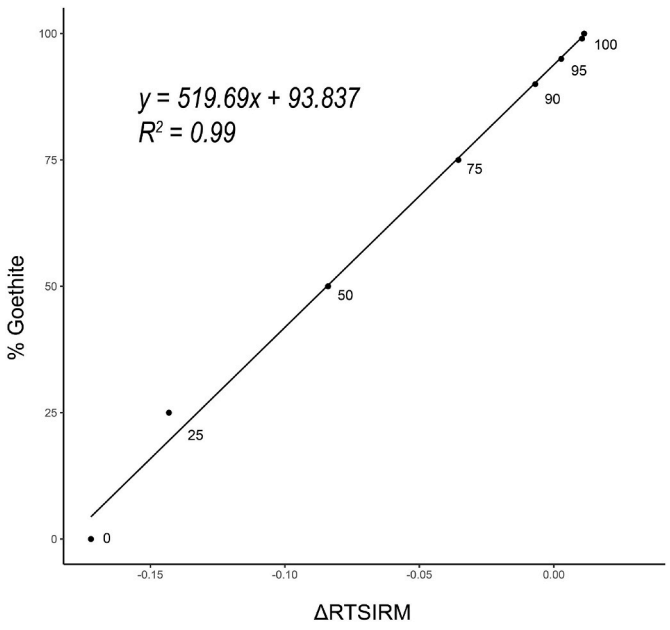

Fig. 4. Calibration curve showing the linear relationship between the percentage goethite present in the mixture and the difference between the magnetic moment at 10K and 300K (ΔRT-SIRM) in the RT-SIRM cooling experiment.

mT; however, Liu et al. (2006) reported that for content >11–13 mol% Al, the opposite effect is observed and coercivity sharply drops below 100 mT as particle sizes approach ultrafine superparamagnetic sizes. The Al-goethite sample presented in this study has a low coercivity of 68.8 mT (Table 2), which can likely be attributed to high Al substitution in the commercial sample. This is supported by quantitative XRD which suggests approximately 31 % of the bulk sample can be attributed to Al-goethite (Appendix B).

Analysing the mixtures of synthesised hematite and goethite reveal that at least 90 % goethite is needed to observe a downward sloping effect in RT-SIRMs when mixed with hematite (Fig. 3). Using the difference in magnetic moment (M) between 10K and 300K in the RT-SIRM cooling curve (Δ*RTSIRM*), a linear relationship can be observed (Fig. 4).

$$\Delta RTSIRM = M(10\ K)_{cooling} - M(300\ K)_{cooling}$$

Similar to the RT-SIRM measurements, ZFC-FC measurements qualitatively identify distinct transitions for the main iron oxide components (i.e. magnetite and hematite) in mixed samples. These transitions are often seen most easily in the first derivative functions for ZFC-FC plots, however they can also be observed in the raw data as shown in Fig. 5. The Morin transition for hematite can be observed at 260 K, with the transition visible in concentrations of 5 % or more hematite when mixed with goethite (Figs. 3 and 5). In natural mixtures of hematite and goethite it has been shown that in a 5 mT field, ZFC-FC curves are thermally irreversible (Carbone et al., 2005). The magnetometry results indicate that our hematite and goethite standards are composed of very fine particles of single domain (SD) towards superparamagnetic (SP). The measurements performed in this study did not probe for SP particles specifically, however it is likely that SP particles, if present, do not dominate the magnetic particle assemblage. This is because SP would be expected to return reversible ZFC-FC curves above 30 K and separating below 26 K (Carbone et al., 2005).

3.2. Low-temperature behaviour of natural ochre pigments

The calibration curve developed (Fig. 6) to determine semi-quantitative amounts of goethite is a proof of concept for further work in this area, whereby magnetic measurements could be used to deconvolute mixtures based on quantitative measures rather than only qualitative observations. The application of this model is best suited as supplementary to other qualitative assessments, and when applied to goethite dominant samples, can give an indication for the goethite content.

The linear calibration curve was applied to the measured pigment samples revealing that most of the source samples have a magnetic component characterised as 90–99 % goethite. The use of ΔRTSIRM as a semi-quantitative measure of the goethite concentration in a sample should be used cautiously on samples which do not display a clear goethite shape and instead is best used in conjunction with qualitative observations. The samples that indicate goethite character >100 % synthetic goethite can be attributed to Al-substitution due to the qualitative similarities in the RT-SIRM and ZFC-FC measurements for those samples and the measured Al-goethite standard. As shown in Fig. 2, the presence of Al-goethite results in an RT-SIRM plot which appears qualitatively similar in shape to goethite, with a subtle feature around 280 K, however the remanent magnetisation is significantly higher. This increase in bulk magnetisation is due to the unbalanced moments resulting from the clustering of aluminium ions along the sublattice (Dekkers, 1989; Pollard et al., 1991).

One challenge of using mineral magnetic measurements is that magnetite is known to dominate the response in a mixture, where even small amounts of magnetite can obscure the presence of other minerals (Liu et al., 2012, 2019). One method to partially overcome the dominance of magnetite is to use enhanced SIRMs (Fig. 7), which allow for the identification of goethite, if present, by sampling a higher temperature range (up to 400 K) even if unobservable in a traditional RT-SIRM. As shown in Fig. 7, the initial cooling (blue) and warming (red) curves show some hematite character, however once the demagnetisation occurs at 400 K the following cooling and warming curves become almost reversible, suggesting the presence of goethite. This temperature is high enough to impart a thermal remanent magnetisation (TRM) onto the goethite components as the sample cools through the Neél temperature (~393 K) when exposed to a magnetic field. This produces a distinct response which can easily be interpreted to determine the presence or absence of goethite when other qualitative assessments may be ambiguous (Lagroix and Guyodo, 2017).

3.2.1. Analysis of archaeological sources

Hysteresis, RT-SIRM and ZFC-FC measurements were performed for a subset of samples from each study site to identify (1) the degree of variation between sites and (2) the variation within sites and the subsites. This resulted in plots from which the key parameters could be summarised as per Table 2 (Appendix D, Table 1). The subset of this dataset presented here (Figs. 7–10 and Table 3) shows the dominance of goethite in most cases, as well as the presence of other iron oxides such as hematite and magnetite.

The interpretation of the hysteresis loops is done by evaluating how open the loop is, as this relates to the coercivity (B_c) of the minerals. Low coercivity ferrimagnetic minerals produce narrow loops (e.g. magnetite), while high coercivity antiferromagnetic minerals create more open loops (e.g. hematite) (Mooney et al., 2003). For hematite, B_c is typically >100–300 mT, goethite is less coercive, and magnetite and maghemite are the least (Liu et al., 2012). Nearly straight and closed loops are characteristic of goethite (Lagroix and Guyodo, 2017). Wasp-waisted

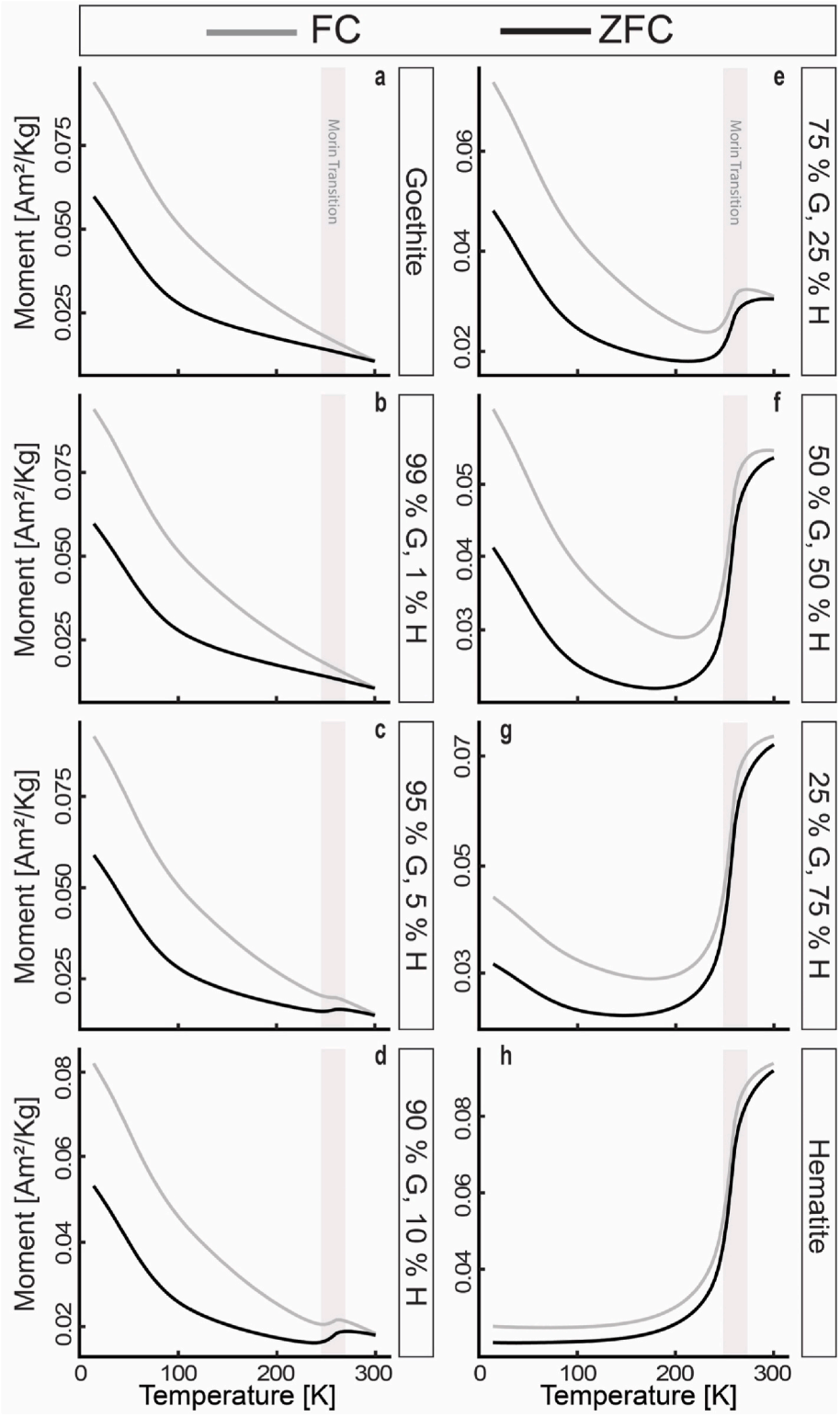

Fig. 5. ZFC-FC curves for goethite and hematite mixtures.

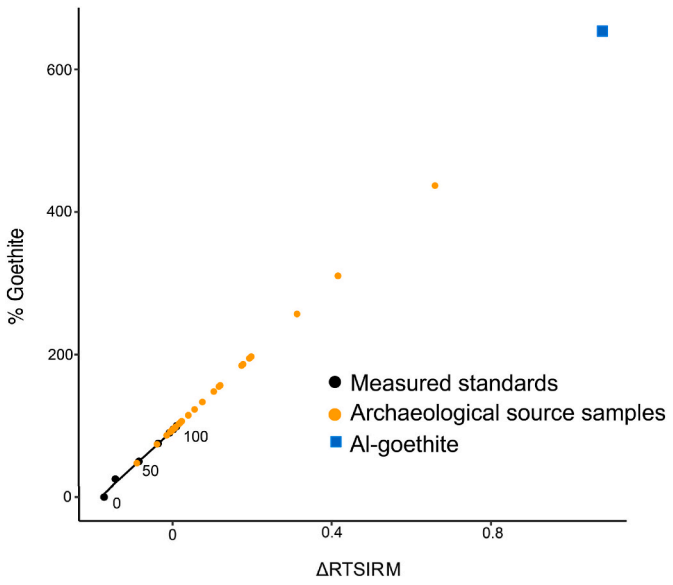

Fig. 6. Calibration curve for the RT-SIRM standard measurements (black), Al-goethite (blue) and archaeological source samples (orange). (For interpretation of the references to colour in this figure legend, the reader is referred to the Web version of this article.)

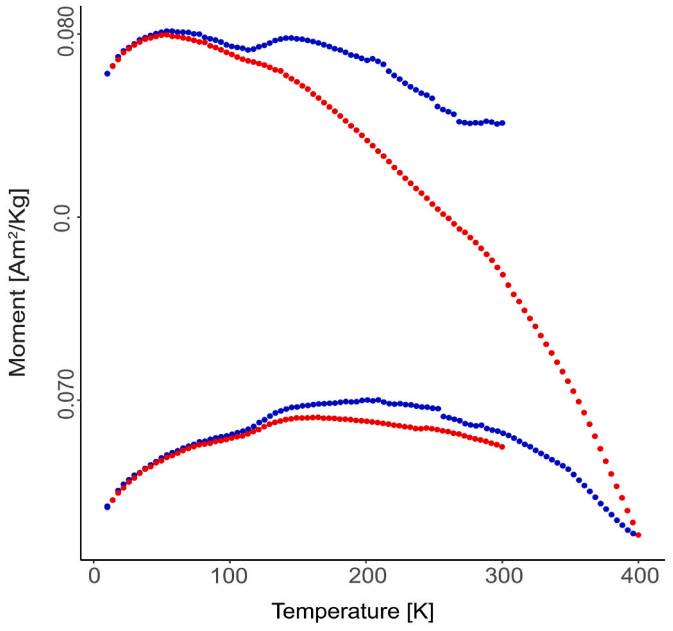

Fig. 7. Enhanced SIRM measurement for sample KEN034 demonstrating the ability to qualitatively identify goethite in a hematite or magnetite dominant sample.

loops are interpreted as being the result of magnetic grains having extremely different coercivities (Zhang et al., 2016). Pot-bellied loops are those where the width of the loop becomes broader approaching zero, and then closes again. These are interpreted as there being at least two minerals, where at least one has a much higher coercivity (Bennett and Della Torre, 2005).

The interpretation of the RT-SIRM and ZFC-FC curves is done by identifying the dominant shape (Fig. 3) and by identifying any transitions that may be present (Table 3). The colour of the ochres measured (Table 3) are provided supplementary to the mineralogical assessment. While colour is an important parameter to consider, it is also difficult to control and therefore less accurate than the mineralogical assignments used for fingerprinting.

The Overland Corner (OVR) samples (Fig. 8), associated with strongly pigmented ochres on Tertiary sandstone (Table 1) are characterised by low (Fig. 8a) to high (Fig. 8d) coercivity hysteresis loops and low temperature vs moment shapes resembling goethite and hematite. While OVR-a-1-919 displays characteristic goethite features in the RT-SIRM, OVR-a-5-0421 displays changes near the Morin transition, with shapes resembling hematite (Fig. 2) as well as pot-bellied hysteresis typical of SD-SP mixtures (Tauxe et al., 1996).

White Cockatoo (WCO) samples, taken from surficial ferricrete on Cretaceous weathering profile (Table 1) are characterized by wasp-waisted hysteresis loops (Fig. 9a–d) indicating magnetic mineral mixtures of different coercivities (Tauxe et al., 1996). The temperature vs moment curves (Fig. 9b, c, e, f) resemble the shapes of goethite, hematite and magnetite (Fig. 2) in varying degrees. While some samples are dominated by goethite, as evidenced by high magnetic moment at low temperatures and almost reversible RT-SIRM (e.g., WCO-e-1-819; Fig. 9), other samples display both the Verwey transition of magnetite and the Morin transition of hematite (e.g., WCO-a-1-819; Fig. 9).

The Tom Price (RR, WADP and WARE) samples are all from three different ochre outcrops of Proterozoic Banded Iron Formations (BIFs) (Table 1) and therefore each has unique magnetic signals. A striking feature of the RR site is the cation substitution in goethite. The RR sample (Fig. 10a–c) is predominantly goethite in character with clear indications for the presence of Al-goethite, sharing the same distinctive features as the Al-goethite sample presented in Fig. 6. This includes the subtle change in slope at 250 K in the RT-SIRM and the approach to asymptote beginning at 260 K in the ZFC-FC measurement. WADP07 also likely contains Al-goethite due to the high ΔRTSIRM value and high moment (Fig. 10e), however an alternative explanation for this would be the presence of maghemite which would increase the overall bulk magnetisation. WARE is once again characterised by the distinct goethite signal, however there is evidence for the presence of hematite in the RT-SIRM and hysteresis loop (Fig. 10g and h).

The Kenyan (KEN) samples (Fig. 11), taken from weathered volcanic deposits are interpreted as largely goethite dominant (Fig. 10d–f). KEN001 (Fig. 11a–c) exhibits the downward sloping effects in the RT-SIRM, which can be associated with the presence of goethite however the overall shape observed cannot be attributed to goethite, hematite or magnetite alone. The low coercivity hysteresis loop, shapes of thermomagnetic curves with non-reversible RT-SIRM and FC above the ZFC closing near T_V clearly indicates the likely presence of an iron oxide not represented in the measured standards such as maghemite.

The dominance of goethite in the ochres presented is not all that surprising as the formation of goethite in oxidising soils occurs ubiquitously irrespective of climatic environments (Schwertmann, 1993). Similarly, in soils, hematite ordinarily coexists with goethite, and therefore the observation of hematite features (see Fig. 10, sample WARE27-RS-16Y-0821) present in conjunction with a dominant goethite signal is to be expected (Schwertmann, 1993). Hematite can be easily identified in the RT-SIRM due to (1) T_m at 260 K and (2) the bifurcation of the heating and cooling curves at 100 K (see Figs. 8e, 9b and 10h, samples OVR-a-5-0421, WCO-a-1-919 and WARE27-RS-16Y-0821). However, the absence of a hematite signal in

Table 2
Summary of hysteresis and low-temperature properties for standards and mixtures.

Parameter	Units	Magnetite	Al-Goethite[a]	Goethite	99 % Goethite 1 % Hematite	95 % Goethite 5 % Hematite	90 % Goethite 10 % Hematite	75 % Goethite 25 % Hematite	50 % Goethite 50 % Hematite	25 % Goethite 75 % Hematite	Hematite
Mass	mg	3.32	9.59	28.65	28.65	30.54	27.3	35.17	37.14	33.14	35.39
M(7T)	Am^2/kg	6.87×10^{-2}	3.57×10^{-3}	2.26×10^{-3}	2.53×10^{-3}	2.51×10^{-3}	2.33×10^{-3}	2.19×10^{-3}	2.08×10^{-3}	1.84×10^{-3}	1.55×10^{-3}
M_r	Am^2/kg	1.04×10^{-2}	6.91×10^{-5}	1.33×10^{-5}	1.61×10^{-5}	2.35×10^{-5}	3.17×10^{-5}	5.97×10^{-5}	1.08×10^{-4}	1.51×10^{-4}	1.94×10^{-4}
M_r/M(7T)	Dimensionless	1.51×10^{-1}	1.92×10^{-2}	5.87×10^{-3}	6.37×10^{-3}	9.34×10^{-3}	1.36×10^{-2}	2.73×10^{-2}	5.21×10^{-2}	8.17×10^{-2}	1.25×10^{-1}
B_c	mT	26.8	68.8	39	41.7	70.2	87.6	146.3	200.3	230.6	260.2
RT-SIRM (5T)	Am^2/kg	9.22	5.67×10^{-2}	1.02×10^{-2}	1.28×10^{-2}	2.04×10^{-2}	2.86×10^{-2}	5.73×10^{-2}	1.06×10^{-1}	1.48×10^{-1}	1.92×10^{-1}
10K ZFC (5T)	Am^2/kg	9.98	3.59	5.50×10^{-2}	5.98×10^{-2}	5.89×10^{-2}	5.34×10^{-2}	4.84×10^{-2}	4.10×10^{-2}	3.18×10^{-2}	2.09×10^{-2}
10K FC (5T)	Am^2/kg	9.16	3.92	8.66×10^{-2}	9.34×10^{-2}	9.18×10^{-2}	8.25×10^{-2}	7.37×10^{-2}	6.00×10^{-2}	4.42×10^{-2}	2.51×10^{-2}

[a] Corrected for Al-goethite contribution based upon quantitative XRD results (Appendix B and section 2.5.2).

many cases across multiple sites does not preclude the presence of hematite in the ochres, but it is likely that if present, it is in small quantities (less than 1 % of the magnetic component) as determined through the standard mixtures.

In the case of hematite, T_m is generally around 260 K, however it has been shown that with decreasing particle size and/or Al substitution the temperature at which the transition occurs also decreases (Özdemir et al., 2008). Therefore, it can be interpreted that the transitions between 200 and 260 K observed in samples OVR-a-5-0421 and WCO-a-1-919 (Figs. 8e and 9b) are likely due to hematite with a small particle size, however substitution cannot be precluded.

A comparison of all sites shows that each geological setting analysed is magnetically unique from one another while all the sites are characterised by a dominance of goethite. For example, the dominance of goethite character in the hysteresis and RT-SIRM plots for Overland Corner (Fig. 8), while White Cockatoo is characterised by wasp-waisted loops and hematite transitions in the ZFC-FC (Fig. 9). The WA sites represent variability of mineral magnetic properties within the BIFs in the Tom Price area where the RR sample displays clear indications for the presence of Al-goethite, while the WADP and WARE samples can be

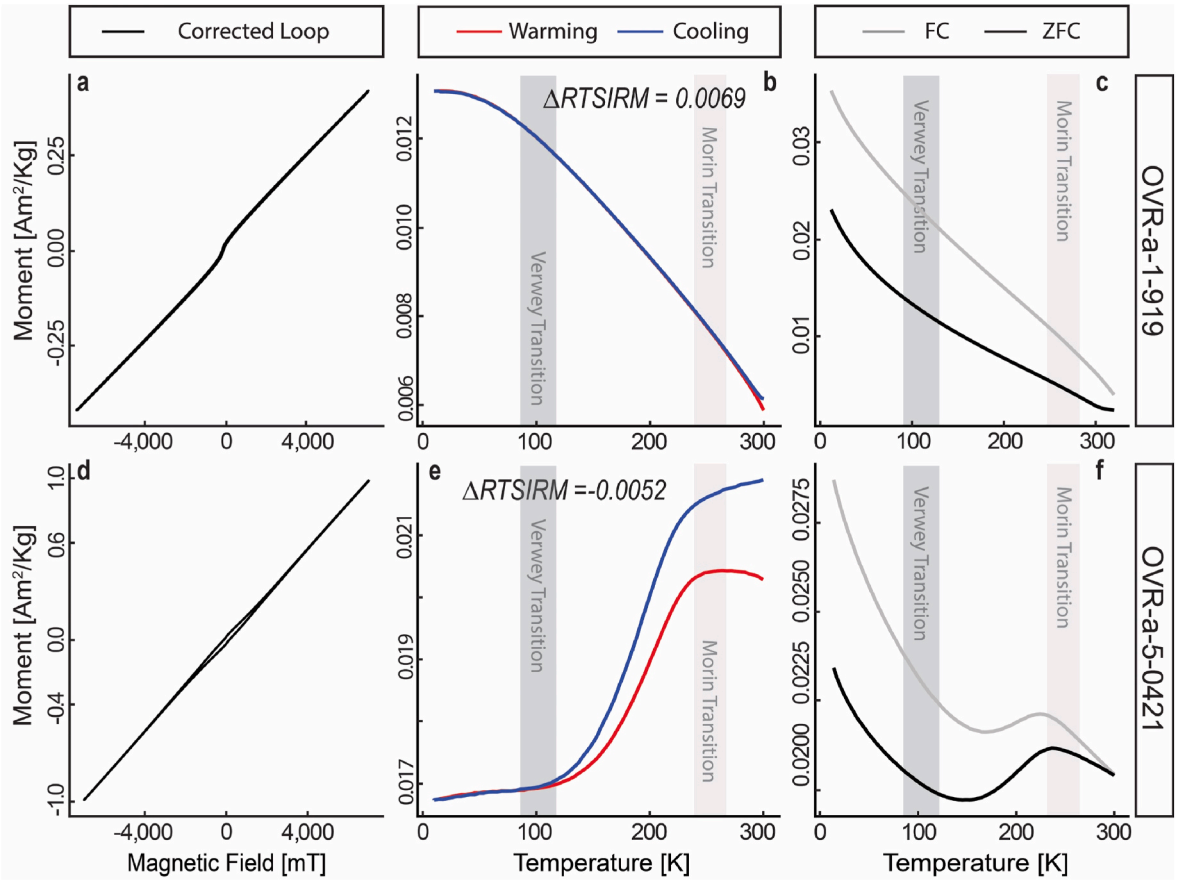

Fig. 8. Representative samples from Overland Corner, South Australia. (a) low-coercivity hysteresis loop, (b) RT-SIRM indicative of goethite (c) ZFC-FC with no transitions, (d) pot-bellied hysteresis loop, (e) RT-SIRM with hematite transition and (f) ZFC-FC with mixed goethite and hematite shape. Grey bars denote the temperature ranges for the Morin transition (241–261 K) (Özdemir et al., 2008) and the Verwey transition (80–125 K) (Jackson and Moskowitz, 2020).

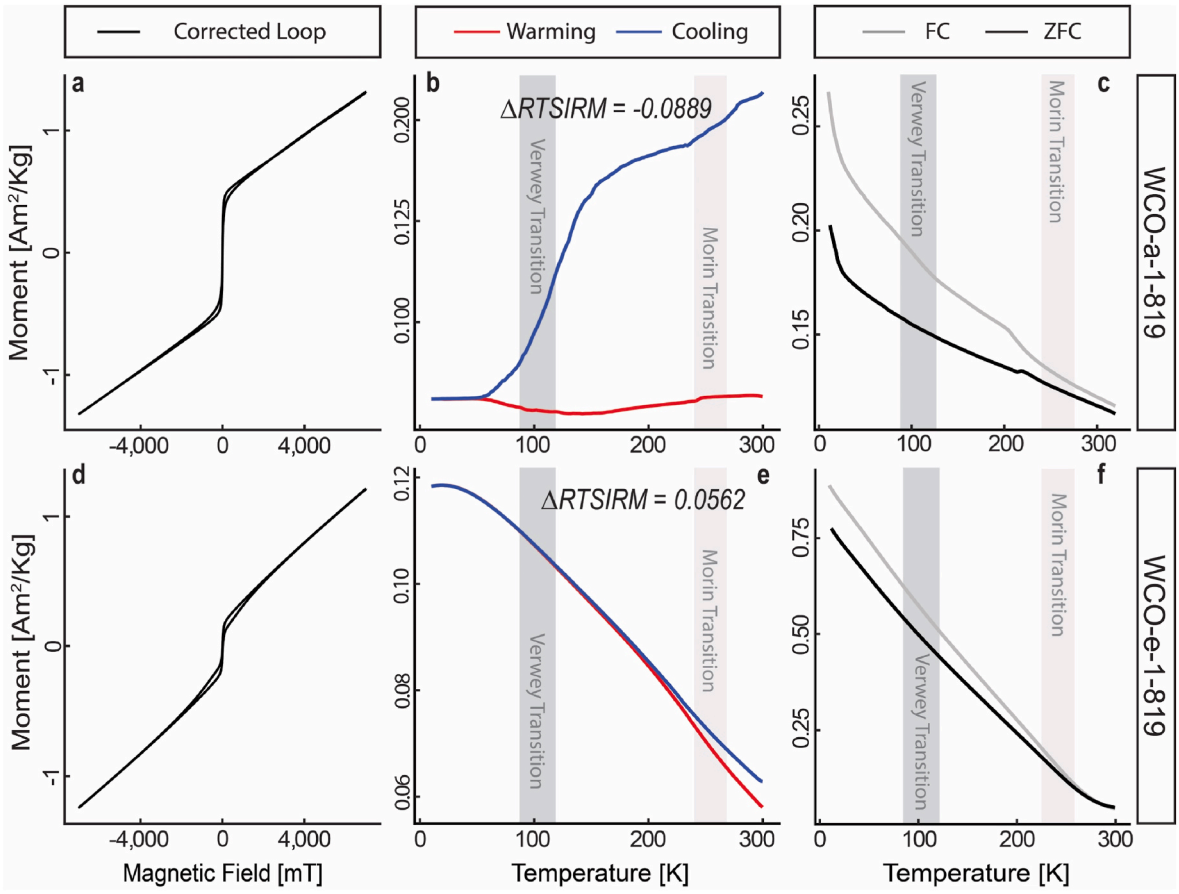

Fig. 9. Representative samples from White Cockatoo, Northern Territory. (a) Wasp-waisted loop, (b) RT-SIRM indicative of magnetite (c) ZFC-FC with hematite transition, (d) wasp-waisted hysteresis loop, (e) RT-SIRM indicative of goethite and (f) ZFC-FC with no transitions. Grey bars denote the temperature ranges for the Morin transition (241–261 K) (Özdemir et al., 2008) and the Verwey transition (80–125 K) (Jackson and Moskowitz, 2020).

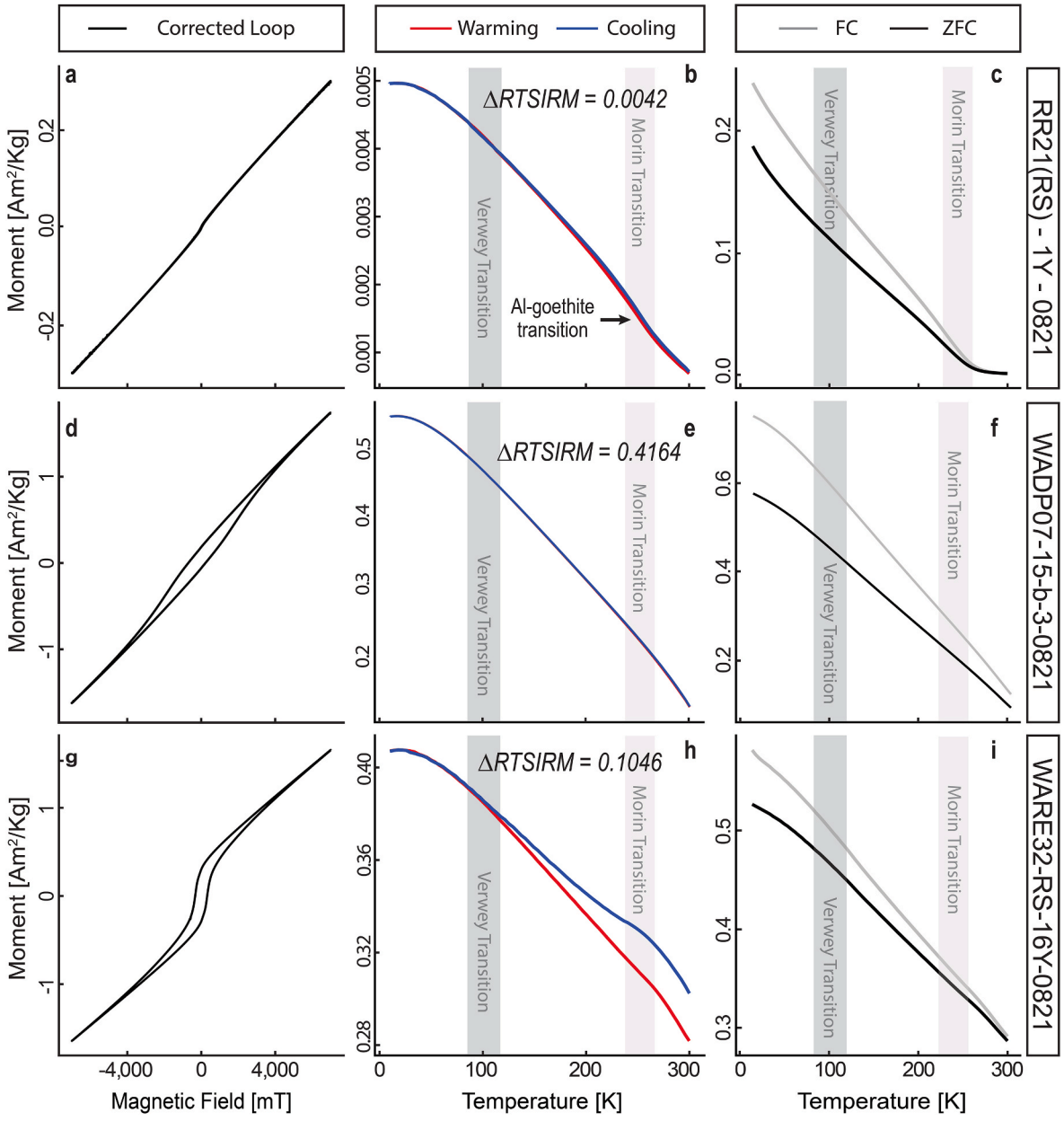

Fig. 10. Representative samples Tom Price, Western Australia. (a) low-coercivity hysteresis loop, (b) RT-SIRM indicative of Al-goethite (c) ZFC-FC with Al-goethite transition, (d) pot-bellied hysteresis loop, (e) RT-SIRM indicative of goethite (f) ZFC-FC with no transitions, (g) wasp-waisted hysteresis loop, (h) RT-SIRM with goethite shape and hematite transition and (i) ZFC-FC with no transitions. Grey bars denote the temperature ranges for the Morin transition (241–261 K) (Özdemir et al., 2008) and the Verwey transition (80–125 K) (Jackson and Moskowitz, 2020).

Table 3
Qualitative interpretation of magnetic measurements for the archaeological ochres.

Sample	Colour (RGB)	Hysteresis	RT-SIRM	ZFC-FC
OVR-a-1-919	*209.2, 130.7, 85.5*	Nearly straight and closed	Goethite shape	No transitions
OVR-a-5-0421	*154.2, 97.3, 75.8*	Low-coercivity	Hematite shape	Transition at 240 K
WCO-a-1-819	118.1, *65.9, 61.4*	Wasp-waisted	Hematite and magnetite shape	Transition at 230 K
WCO-e−1-819	158.1, *94.7, 61.3*	Wasp-waisted	Goethite shape with hematite features	No transition
RR21(RS)-1Y-0821	*232.7, 180, 113.4*	Nearly straight and closed	Al-goethite shape	Al-goethite tail
WADP07-15-b-3-0821	204.5, *128.1, 35.9*	Pot-bellied	Goethite shape	No transition
WARE14-32-RS-16Y-0821	*181.4, 124.1, 74.1*	Wasp-waisted	Dominant goethite shape with hematite features	No transition
KEN001	*181.2, 96.8, 53.8*	Low-coercivity	Goethite shape with unknown features	No transition
KEN021	*171, 94.17, 68.7*	Low-coercivity	Goethite shape with unknown features	No transition

characterised by a high B_c (Fig. 10 and Appendix D, Table 1) and goethite dominance. Both Kenyan samples while characterised by a low-coercivity loop are unique from all other sites presented in the clear influence of another iron oxide type such as maghemite in the RT-SIRM curves (Fig. 11).

The qualitative characterisation of source ochres presented in this manuscript suggests that the magnetic properties are unique to the different geological settings and can be used to characterise the iron mineralogy of the ochre deposits. Goethite is the most abundant and most stable iron hydroxide and can be found in almost all soils (Vodyanitskii, 2010). The formation of hematite is associated with dry, oxidised soils, but also with tropical soils, residual weathering profiles and iron crusts (Maher, 1986). As such, goethite and hematite are commonly found in Australian surface and near-surface geological deposits and soils and is well represented in the presented dataset (Hu et al., 2020). A comparison of the SIRM values from archaeological data presented in this study and the Australian ochre samples from Mooney et al. (2003) reveals comparable SIRM values for all of the samples. For most of the samples, this is not indicative of any regional signal, but rather a result of the varied deposits measured in both studies. Similarities between the Tom Price samples presented here (WADP, WARE and RR) and the Wilgie Mia samples from Mooney et al. (2003) could be indicative of regional similarities, with SIRM values higher for these sites relative to the other measured samples (3.02×10^{-1} and 7.50×10^{-1} Am^2/kg, WARE and WADP respectively) (Appendix D, Table 1). The argument for regional similarities is further supported by Hu et al. (2020) continental-mapping of Australian soils, where parts of Western Australia are characterised by overall higher susceptibility.

While it is postulated that the soil magnetic signal contribution can

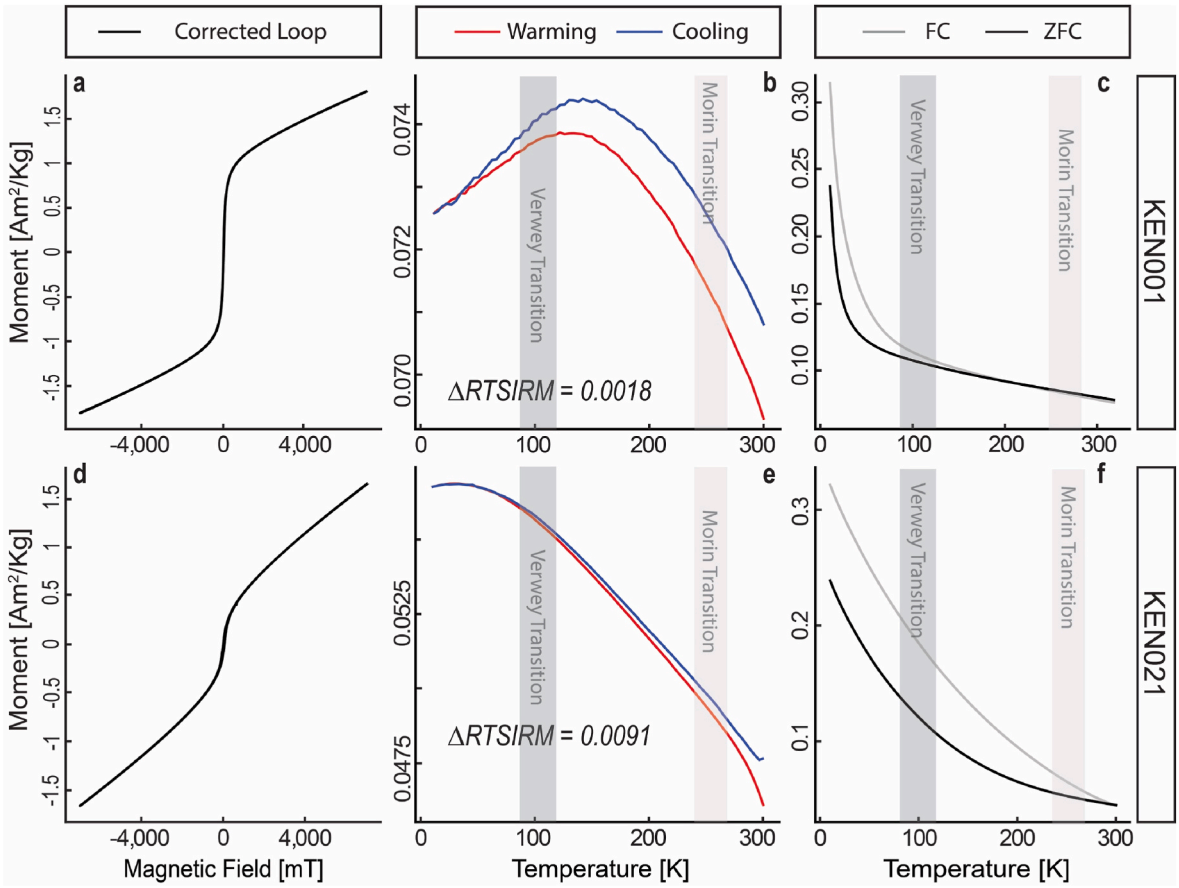

Fig. 11. Representative samples from the Kenyan Rift Valley, Kenya. (a) low-coercivity hysteresis loop, (b) RT-SIRM indicative of goethite (c) ZFC-FC with no features, (d) low-coercivity hysteresis loop, (e) RT-SIRM indicative of goethite (f) ZFC-FC with no transitions. Grey bars denote the temperature ranges for the Morin transition (241–261 K) (Özdemir et al., 2008) and the Verwey transition (80–125 K) (Jackson and Moskowitz, 2020).

in most cases be attributed to magnetite, hematite and goethite (Table 3), other primary and secondary iron-bearing minerals such as maghemite, lepidocrocite and ferrihydrite occur readily in soil deposits and can contribute to the complex magnetic mixtures (Maher, 1986; Mastrotheodoros and Beltsios, 2022). In the case of lepidocrocite, this is unlikely to be found in conjunction with hematite due to the different pedoenvironments needed for formation (Schwertmann, 1993). While most of the ochres measured can be interpreted using the three-mineral model (hematite, goethite and magnetite) due to their strong and distinctive magnetic signals, there is the potential for influences from these other iron oxide types and thus further work is required to be able to identify all iron oxides which may be present. The identification of Al-goethite in the Tom Price samples supports the need to consider elemental substitution within these iron oxides when unmixing magnetic curves (Fitzpatrick and Schwertmann, 1982; Vodyanitskii, 2010). In addition to Al-goethite, Al-hematite is also known to form readily in soils and may contribute to the magnetic responses measured (Cornell and Schwertmann, 2003; Fontes and Weed, 1991; Friedl and Schwertmann, 1996). While qualitative comparisons between sites can be made from the distinctive RT-SIRM curves which are often a strong indicator for the major iron oxides present, the real challenge is the ability to find representative absolute values which can be compared between sites. Data presented in Figs. 8–11 and Table 3 strongly support the assumption that each site has a characteristic set of magnetic properties which can be used to differentiate between the sites. The use of qualitative assessments rather than SIRM and Ms values (parameters provided Appendix D, Table 1) is due to the inherent bias that comes from the mass of the iron component being unknown. When a sample is measured, the magnetisation values are corrected to the mass of sample in the capsule, however in natural ochre samples, the iron content of these ochres can range from 2 to 50+ %, where two ochres from the same site might have identical magnetic properties, however the SIRM and Ms values might be drastically different depending on the concentration of iron oxides present. The qualitative attribution of iron oxides present in ochre samples should be driven by the presence and absence of transitions, the relative intensity of the magnetisation curves and the coercivity of the minerals as these parameters are independent of mass.

4. Conclusion

This proof-of-concept study establishes mineral magnetic measurements as a means to characterise iron-rich minerals from known ochre sources and thus can be part of a larger approach to provenancing cultural and archaeological ochre. The use of the RT-SIRM, ZFC-FC and hysteresis plots together is one part of a multi-proxy approach, where future work could include the combined use of other magnetic measurements such as first-order-reversal-curve (FORC) diagrams or AC-susceptibility, while microscope imagery of the particles can generate a more holistic picture of the overall magnetic properties of samples. In practice, this method could be applied to nodules of ochre that are regularly found in archaeological sites where non-destructive analyses are required. Mineral magnetic measurements have several advantages in that they utilise very small sample sizes (<30 mg), are non-destructive and are immune to the challenges of working with less crystalline materials. Unlike XRD, mineral magnetic measurements have the sensitivity to detect iron oxides such as goethite, even when present in very small quantities (as low as 1 ppm) (Lagroix and Guyodo, 2017), and can be used on ochre in any form, allowing the non-destructive analysis of culturally sensitive materials. The magnetic measurements used in this study allow for the qualitative detection of goethite even in the presence of other magnetically dominating iron oxide phases, which is almost impossible with other conventional analytical methods such as XRD. The novel approach to semi-quantitative data (goethite percentage in mixtures) interpretation uses a simple model to provide insight into the complexity of ochre mixtures, and how greater understanding of the iron oxide mixtures found in natural deposits is required. The interpretation of the hysteresis, RT-SIRM and ZFC-FC results for all samples indicate that all sites can be distinguished from one another using the proposed method. Using the combination of all three measurements, even two sites which may be goethite dominant, can be separated from one another with the use of complementary measurements.

For future work, a larger dataset should be developed to assess the extent of intra-site variation, towards future provenance studies. The combination of RT-SIRM, ZFC-FC and hysteresis measurements is essential for differentiating between archaeological sources. Further studies incorporating ochre from known sources worldwide and within Australia will further develop the capabilities of the method by exploring different proportions of key iron-bearing minerals and therefore refine the ability of the method to discriminate ochre sources.

CRediT authorship contribution statement

Maddison L. Crombie: Writing – review & editing, Writing – original draft, Visualization, Methodology, Investigation, Formal analysis, Data curation, Conceptualization. **Agathe Lisé-Pronovost:** Writing – original draft, Supervision, Methodology, Conceptualization. **Marcus J. Giansiracusa:** Writing – original draft, Supervision, Resources, Methodology, Investigation, Conceptualization. **Colette Boskovic:** Writing – original draft, Supervision, Resources, Methodology, Conceptualization. **Amy Roberts:** Writing – review & editing, Supervision, Funding acquisition. **Felix Lauer:** Writing – review & editing, Formal analysis, River Murray Mallee Aboriginal Corporation, Resources. **Rachel S. Popelka-Filcoff:** Writing – review & editing, Writing – original draft, Supervision, Resources, Methodology, Investigation, Formal analysis, Data curation, Conceptualization.

Declaration of competing interest

The authors declare the following financial interests/personal relationships which may be considered as potential competing interests:

Rachel Popelka-Filcoff, Maddison Crombie, Agathe Lisé-Pronovost, Marcus J. Giansiracusa, Colette Boskovic, and Amy Roberts report financial support was provided by Australian Research Council. Rachel Popelka-Filcoff is on the editorial board of Journal of Archaeological Science. If there are other authors, they declare that they have no known competing financial interests or personal relationships that could have appeared to influence the work reported in this paper.

Acknowledgements

The work has been approved by the Human Ethics Committee Ethics approval number 8408/2013 from the Social and Behavioural Research Ethics Committee of Flinders University and 14478/2057611 from the Human Research Ethics Committees of University of Melbourne. This research was supported partially by the Australian Government through the Australian Research Council's *Discovery Projects* funding scheme (project DP190102219). Maddison Crombie was supported by an Australian Government Research Training Programme Scholarship provided by the Commonwealth of Australia and the University of Melbourne. Dr Agathe Lisé-Pronovost is the recipient of an Australian Research Council Discovery Early Career Researcher Award (DE230100721). Dr Marcus Giansiracusa is the recipient of a Melbourne Postdoctoral Fellowship from the University of Melbourne. Professor Amy Roberts is the recipient of an Australian Research Council Future Fellowship (FT230100499) funded by the Australian Government. For the Overland Corner samples, we acknowledge 1) RMMAC members and Flinders University students for their assistance in the field and 2) the South Australian Government's Department of Environment and Water (Crown Lands Program) and Aboriginal Affairs and Reconciliation (Department of Premier and Cabinet) for assistance with access and research permits. For the Barunga samples, we acknowledge Jawoyn (Barunga) Junggayi and Traditional Owners. For the Tom Price samples,

we acknowledge the Yinhawangka and Wintawari Guruma people and Dr Caroline Mather. This work was performed in part at the Trace Analysis for Chemical, Earth and Environmental Sciences (TrACEES) Platform at the University of Melbourne. We acknowledge the Australian Research Council for an equipment grant (LE210100009). The authors acknowledge use of the facilities within the Monash X-ray Platform for all Co-XRD analysis. We would like to thank Dr Andrew Zipkin for providing samples from Kenya used in the study and Professor Allan Pring for providing the magnetite sample from the South Australian Museum and Dr Venera May and Noa Abrahams for assistance with preparation of ochre samples. We would also like to thank Dr Nithin Suryadevara for assistance in the lab.

Appendix A. Supplementary data

Supplementary data to this article can be found online at https://doi.org/10.1016/j.jas.2025.106222.

References

Barham, L., 2002. Systematic pigment use in the middle pleistocene of south-central Africa. Curr. Anthropol. 43, 181–190.
Bennett, L.H., Della Torre, E., 2005. Analysis of wasp-waist hysteresis loops. J. Appl. Phys. 97.
Carbone, C., Di Benedetto, F., Marescotti, P., Sangregorio, C., Sorace, L., Lima, N., Romanelli, M., Lucchetti, G., Cipriani, C., 2005. Natural Fe-oxide and-oxyhydroxide nanoparticles: an EPR and SQUID investigation. Mineral. Petrol. 85, 19–32.
Cornell, R.M., Schwertmann, U., 2003. The Iron Oxides: Structure, Properties, Reactions, Occurrences, and Uses. Wiley-vch Weinheim.
Dekkers, M.J., 1989. Magnetic properties of natural goethite-I. Grain-size dependence of some low- and high-field related rockmagnetic parameters measured at room temperature. Geophys. J. Int. 97, 323–340.
Dunlop, D.J., 2002. Theory and application of the Day plot (M/M versus H/H) 2. Application to data for rocks, sediments, and soils. J. Geophys. Res. Solid Earth 107. EPM 5-1-EPM 5-15.
Dunlop, D.J., Özdemir, Ö., 1997. Rock Magnetism: Fundamentals and Frontiers. Cambridge University Press, Cambridge.
Fitzpatrick, R.t., Schwertmann, U.v., 1982. Al-substituted goethite—an indicator of pedogenic and other weathering environments in South Africa. Geoderma 27, 335–347.
Fontes, M., Weed, S., 1991. Iron oxides in selected Brazilian oxisols: I. Mineralogy. Soil Sci. Soc. Am. J. 55, 1143–1149.
Friedl, J., Schwertmann, U., 1996. Aluminium influence on iron oxides: XVIII. The effect of Al substitution and crystal size on magnetic hyperfine fields of natural goethites. Clay Miner. 31, 455–464.
Hodgskiss, T., 2020. Ochre Use in the Middle Stone Age, Oxford Research Encyclopedia of Anthropology. Oxford University Press Oxford.Hu, P., Heslop, D., Rossel, R.A.V., Roberts, A.P., Zhao, X., 2020. Continental-scale magnetic properties of surficial Australian soils. Earth Sci. Rev. 203, 103028.
Jackson, M.J., Moskowitz, B., 2020. On the distribution of Verwey transition temperatures in natural magnetites. Geophys. J. Int. 224, 1314–1325.
Jaiswal, A., Banerjee, S., Mani, R., Chattopadhyaya, M., 2013. Synthesis, characterization and application of goethite mineral as an adsorbent. J. Environ. Chem. Eng. 1, 281–289.
Klein, C., Gole, M.J., 1981. Mineralogy and petrology of parts of the Marra Mamba iron formation, Hamersley basin, Western Australia. Am. Mineral. 66, 507–525.
Kosterov, A., 2003. Low-temperature magnetization and AC susceptibility of magnetite: effect of thermomagnetic history. Geophys. J. Int. 154, 58–71.
Kukkonen, I.T., Miettinen, M., Julkunen, A., Mattsson, A., 1997. Magnetic prospecting of Stone Age red ochre graves with a case study from Laukaa, central Finland. Fennosc. Archaeol. XIV, 3–12.
Lagroix, F., Guyodo, Y., 2017. A new tool for separating the magnetic mineralogy of complex mineral assemblages from low temperature magnetic behavior. Front. Earth Sci. 5, 61.
Lassoued, A., Dkhil, B., Gadri, A., Ammar, S., 2017. Control of the shape and size of iron oxide (α-Fe2O3) nanoparticles synthesized through the chemical precipitation method. Results Phys. 7, 3007–3015.
Liu, P., Hirt, A.M., Schüler, D., Uebe, R., Zhu, P., Liu, T., Zhang, H., 2019. Numerical unmixing of weakly and strongly magnetic minerals: examples with synthetic mixtures of magnetite and hematite. Geophys. J. Int. 217, 280–287.
Liu, Q., Roberts, A.P., Larrasoaña, J.C., Banerjee, S.K., Guyodo, Y., Tauxe, L., Oldfield, F., 2012. Environmental magnetism: principles and applications. Rev. Geophys. 50.
Liu, Q., Yu, Y., Torrent, J., Roberts, A.P., Pan, Y., Zhu, R., 2006. Characteristic low-temperature magnetic properties of aluminous goethite [α-(Fe, Al) OOH] explained. J. Geophys. Res. Solid Earth 111.
Maher, B., 1986. Characterisation of soils by mineral magnetic measurements. Phys. Earth Planet. Inter. 42, 76–92.
Mastrotheodoros, G.P., Beltsios, K.G., 2022. Pigments—iron-based red, yellow, and brown ochres. Archaeol. Anthropol. Sci. 14, 1–25.
Mooney, S., Geiss, C., Smith, M., 2003. The use of mineral magnetic parameters to characterize archaeological ochres. J. Archaeol. Sci. 30, 511–523.
Morin, F., 1950. Magnetic susceptibility of αFe_2O_3 and αFe_2O_3 with added titanium. Phys. Rev. 78, 819.
Özdemir, Ö., Dunlop, D.J., 2014. Hysteresis and coercivity of hematite. J. Geophys. Res. Solid Earth 119, 2582–2594.
Özdemir, Ö., Dunlop, D.J., Berquó, T.S., 2008. Morin transition in hematite: size dependence and thermal hysteresis. Geochem. Geophys. Geosyst. 9.
Özdemir, Ö., Dunlop, D.J., Moskowitz, B.M., 1993. The effect of oxidation on the Verwey transition in magnetite. Geophys. Res. Lett. 20, 1671–1674.
Pálsdóttir, A.H., Bläuer, A., Rannamäe, E., Boessenkool, S., Hallsson, J.H., 2019. Not a limitless resource: ethics and guidelines for destructive sampling of archaeofaunal remains. R. Soc. Open Sci. 6, 191059.
Paterson, G.A., Zhao, X., Jackson, M., Heslop, D., 2018. Measuring, processing, and analyzing hysteresis data. G-cubed 19, 1925–1945.
Peters, C., Dekkers, M., 2003. Selected room temperature magnetic parameters as a function of mineralogy, concentration and grain size. Phys. Chem. Earth, Parts A/B/C 28, 659–667.
Pickard, A., 2002. SHRIMP U–Pb zircon ages of tuffaceous mudrocks in the Brockman iron formation of the Hamersley range, Western Australia. Aust. J. Earth Sci. 49, 491–507.
Pollard, R., Pankhurst, Q., Zientek, P., 1991. Magnetism in aluminous goethite. Phys. Chem. Miner. 18, 259–264.
Popelka-Filcoff, R.S., Robertson, J.D., Glascock, M.D., Descantes, C., 2007. Trace element characterization of ochre from geological sources. J. Radioanal. Nucl. Chem. 272, 17–27.
Popelka-Filcoff, R.S., Zipkin, A.M., 2022. The archaeometry of ochre sensu lato: a review. J. Archaeol. Sci. 137, 105530.
Qian, Y., Heslop, D., Roberts, A.P., Hu, P., Zhao, X., Liu, Y., Li, J., Grant, K.M., Rohling, E. J., 2021. Low-temperature magnetic properties of Marine sediments—quantifying magnetofossils, superparamagnetism, and maghemitization: Eastern mediterranean examples. J. Geophys. Res. Solid Earth 126.
Roberts, A.L., Popelka-Filcoff, R., Westell, C., Murray, R., Corporation, M.A., 2022. Ochre, flint and violence: an Aboriginal history of the Ma:ko region (Overland Corner). Trans. Roy. Soc. S. Aust. 146, 319–340.
Schwertmann, U., 1993. Relations between iron oxides, soil color, and soil formation. Soil color 31, 51–69.
Sweet, I.P., Kruse, P.D., Pillinger, D.M., Pieters, P.E., Crick, I.H., 1994. Katherine, Northern Territory : Sheet SD5309. Australian Geological Survey Organisation.
Tauxe, L., Mullender, T., Pick, T., 1996. Potbellies, wasp-waists, and superparamagnetism in magnetic hysteresis. J. Geophys. Res. Solid Earth 101, 571–583.
Tsatskin, A., Gendler, T.S., 2016. Identification of “red ochre” in soil at Kfar HaHoresh Neolithic site, Israel: magnetic measurements coupled with materials characterization. J. Archaeol. Sci.: Report 6, 284–292.
Vodyanitskii, Y.N., 2010. Iron hydroxides in soils: a review of publications. Eurasian Soil Sci. 43, 1244–1254.
Ward, I., Watchman, A., Cole, N., Morwood, M., 2001. Identification of minerals in pigments from aboriginal rock art in the Laura and Kimberley regions, Australia. Rock Art Research 18, 15–23.
Wolf, S., Conard, N.J., Floss, H., Dapschauskas, R., Velliky, E., Kandel, A.W., 2018. The use of ochre and painting during the Upper Paleolithic of the Swabian Jura in the context of the development of ochre use in Africa and Europe. Open Archaeol. 4, 185–205.
Zhang, R., Necula, C., Heslop, D., Nie, J., 2016. Unmixing hysteresis loops of the late Miocene–early Pleistocene loess-red clay sequence. Sci. Rep. 6, 29515.
Zipkin, A.M, Hanchar, J., Brooks, A.S., Grabowski, M., Thompson, J., Gomani-Chindebvu, E., 2015. Ochre fingerprints: distinguishing among Malawian mineral pigment sources with homogenized ochre chip LA–ICPMS. Archaeometry 57, 297–317.
Zipkin, A.M., Ambrose, S.H., Hanchar, J.M., Piccoli, P.M., Brooks, A.S., Anthony, E.Y., 2017. Elemental fingerprinting of Kenya Rift Valley ochre deposits for provenance studies of rock art and archaeological pigments. Quat. Int. 430, 42–59.